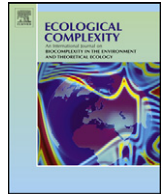




Contents lists available at [ScienceDirect](http://www.sciencedirect.com)

Ecological Complexity

journal homepage: www.elsevier.com/locate/ecocom



The structure of ecological state transitions: Amplification, synchronization, and constraints in responses to environmental change

Jonathan D. Phillips*

Tobacco Road Research Team, Department of Geography, University of Kentucky, Lexington, KY 40506-0027, United States

ARTICLE INFO

Article history:

Received 24 February 2011
Received in revised form 20 July 2011
Accepted 22 July 2011
Available online xxx

Keywords:

State-and-transition models
Spectral radius
Algebraic connectivity
S-metric
Ecological response
Climate change
Synchronization

ABSTRACT

Effects of environmental change may be either amplified and facilitated, or constrained, by the network of state-changes in ecological systems. Network structure affects system response independently of the dynamics of the individual subsystems. Ecological responses were represented as state-and-transition models (STMs), and analyzed as mathematical graphs. Three metrics were applied that reflect: (1) the extent to which environmental change is amplified or filtered by state transitions; (2) network synchronizability and the rate of propagation of state changes; and (3) the extent of system structural constraints to the spatial propagation of state transitions. These were determined for seven archetypal graph structures representing common forms of connectivity in ecological networks, and linked to distinct modes of ecological change. Radiation-type structures are the least synchronized and most constrained patterns, with the most limited amplification, followed by other low-connectivity patterns such as those associated with monotonic succession. The maximum-connectivity rigid polygon structure (any state can transition to any other) has the strongest amplification and synchronization and least constraints. Structural constraints to change propagation are most sensitive to increasing numbers of transitions for a given number of states, and synchronization also increases at least linearly with the number of links. Amplification, however, does not increase as rapidly; as long as a graph is connected, increasing the number of links does not proportionally increase it. Because the more densely connected structures have much higher synchronization than other patterns, and fewer constraints on change propagation, environments characterized by these types of STMs may be prone to rapid, complex transitions in response to environmental changes. STMs for rangelands in two regions of Texas show that the rigid polygon structure is very common. If this phenomenon is more general, it suggests that relatively abrupt landscape reorganizations may be more likely than more orderly successions of change along environmental gradients. This analysis shows that identification of STMs and their network structure is useful for recognizing environments at higher risk for complex reorganization, and for identification of management actions to either retard or facilitate propagation of state changes.

© 2011 Elsevier B.V. All rights reserved.

1. Introduction

Ecological responses to climate change, at levels ranging from species to biomes, are typically interpreted or modeled in terms of ranges of tolerance and optimality with respect to temperature, moisture balance, sunlight, etc. These are widely understood to be only first-order controls, however, with changes in ranges, distributions, and boundaries partly determined by other environmental controls and edaphic factors, as well as by dispersal mechanisms and biological interactions (c.f. Westoby et al., 1989; Kupfer and Cairns, 1996; Iverson and Prasad, 2001, 2002; Burkett et al., 2005; Svenning and Skov, 2005; Liang and Schwartz, 2009). Because climate change can indirectly influence hydrological and

geomorphological processes, disturbance regimes, and land management as well as ecological processes, and because other environmental changes may occur concurrently with but independently of climate change, it is appropriate to consider potential ecological responses to change more generally.

At the community, ecosystem, or landscape scale, ecological changes can be represented via state-and-transition models (STMs). These have been most commonly used in range ecology (see overviews by Briske et al., 2005; Bestelmeyer et al., 2009), but have been increasingly applied in ecosystem science more generally (e.g., van der Wal, 2006; Hernstrom et al., 2007; Czembor and Vesk, 2009; Zweig and Kitchens, 2009; Phillips, 2011). A STM identifies potential system states, represented by, e.g., vegetation communities or wetland types, and the possible transformations among them. The conditions driving or favoring these transformations are typically determined based on theoretical or empirically determined probabilities, or on ecologically based rules or

* Tel.: +1 859 257 6950.
E-mail address: jdp@uky.edu.

principles. STMs were developed as an alternative to classical deterministic succession models, but linear successions, as well as random models, are special cases of STMs. The STM approach is consistent with an approach to ecosystem responses to climate change that recognizes disproportionate, nonlinear responses and complex, adaptive landscapes (Burkett et al., 2005; Ryan et al., 2007). This study is also consistent with the topological approach to ecology described by Prager and Reiners (2009).

STMs are typically used to link ecological theory and/or observations to ecosystem management and restoration, or as tools to model, predict, or describe ecological changes based on prior knowledge of processes or phenomena (Bestelmeyer et al., 2009; Zweig and Kitchens, 2009). Predictive applications have largely focused on individual states and transitions. Recently, however, spatial patterns of alternative states and transitions among them have received attention (Bestelmeyer et al., 2011; Phillips, 2011).

Following earlier work (Phillips, 2011), graph theory is used to analyze STM structure. Applications of graph theory to spatial problems in landscape ecology go back at least to the early 1990s (Cantwell and Forman, 1993), and applications to other aspects of ecology and geography go back much further. However, the approach is unfamiliar enough to most environmental scientists that introductions to basic graph theory concepts are given in many recent papers (e.g., Tremi et al., 2008; Urban et al., 2009). Previous applications dealt primarily with issues of connectivity and centrality of spatial elements, and dispersal mechanisms or movement pathways (e.g., Cantwell and Forman, 1993; Bunn et al., 2000; Arlinghaus et al., 2002; Bode et al., 2008; Tremi et al., 2008; Urban et al., 2009; Padgaham and Webb, 2010). This study, by contrast, is concerned with properties of ecological state transition networks related to the ease with which transitions can be spread.

A STM based on transitions among community or higher-level system states can be considered as a network (the system states) composed of a number of individual subnetworks, the interactions among species and between biota and abiotic factors within the states. Restrepo et al. (2006) showed that for such a network, where each individual subnetwork is an oscillator with its own characteristic frequency, there exists a critical coupling strength k_c at which systems undergo a transition from incoherent to coherent behavior. For a large class of dynamical systems and network topologies of this nature Restrepo et al. (2006) showed that

$$k_c = \frac{\mu}{\lambda_1} \quad (1)$$

where λ_1 is the largest eigenvalue of the adjacency matrix of the network (a major determinant of many system properties; Biggs, 1994; Arlinghaus et al., 2002; Restrepo et al., 2006, 2007; Duan et al., 2009) and μ depends on the dynamics of the individual subnetworks. Thus, the dynamics within and between the system states influence overall system behavior independently. This supports the notion that knowledge of the STM structure provides useful information independently of the details of the ecological interactions (and, of course, vice versa).

This is a specific case of the general principle that ecological interactions operating at distinctly different scales are independent with respect to their effects on whole system behavior, as shown by Schaffer (1981) for species interactions, and generalized to a broad class of environmental systems by Phillips (1995).

2. State-and-transition networks

System states and the transitions among them represent a type of network, and as such have associated graphs. Transitions among semi-arid vegetation communities, for example, are typically driven by factors such as climate change, indirect effects of climate change (e.g., fire frequency; grazing pressure), and human land use and

management decisions (e.g., controlled burns or fire suppression; grazing intensity; brush management; plantings) (Bestelmeyer et al., 2009; Briske et al., 2005). Transitions among deltaic soil/geomorphic states may be triggered by drivers such as sea-level and freshwater inflow changes, and geomorphic processes such as sedimentation and avulsions (Phillips, 2011). The states are the nodes or vertices of the graph, and transitions are the links among the nodes.

Graph theoreticians, as well as geographers, engineers, etc. applying graph theory to practical problems, have identified some standard or archetypal graph patterns of mathematical interest, or of special interest to particular applications such as transportation and communication networks (Arlinghaus et al., 2002). Phillips (2011) identified some graph structures treated as endpoints with respect to modes of spatial change in landscapes. All four of these are part of a larger group of seven common, archetypal structures in landscape graphs based on spatial configurations of, and interactions between, landscape elements identified by Cantwell and Forman (1993).

The “necklace” structure (termed a linear sequential STM by Phillips, 2011) is a classic succession-type form; i.e., state A leads to B leads to C and so on. Phillips (2011) recognized a cyclical sequential variant that has an essentially circular structure, termed a “graph cell” by Cantwell and Forman (1993). The “spider” graph of Cantwell and Forman (1993; radiation in Phillips’ 2011 terminology) has a single key or starting state connected to all of the other states, which are connected only to the central or key state. The “cross” form is essentially a hybrid of the graph cell and spider types (Cantwell and Forman, 1993). A fully connected graph where each state is connected to all others is termed a “rigid polygon.” The “candelabra” structure is a variant of the spider, with a specific starting point/state leading to a key or central state connected to all other states. A “mesh” graph is a set of highly connected nodes, but not fully connected as in a rigid polygon (Cantwell and Forman, 1993). These seven graph types are shown in Fig. 1.

A linear sequential or necklace structure represents a successional sequence or a systematic pattern of changes along an environmental gradient. The cyclical sequential graph represents a circular progression, as for example when disturbance periodically resets successional sequences. The spider (radiation) graph could indicate at least two different phenomena – divergent change where a single ecosystem state could be altered into several different states, or convergent change where several different states may be altered to a single state. The former could be associated with, e.g., fragmentation and increased patchiness; the latter with, e.g., a successful invasive species or community. A rigid polygon or maximum connectivity graph could represent a tightly knit, path dependent relationship among states, where a given state could transition to any of the others depending on initial conditions or variations in disturbance. The rigid polygon can also represent a random STM, where any state can transition to any other with equal probability. A cross structure is indicative of a tightly connected pattern, but with some structural constraints (i.e., many transitions are possible, but some are impossible). Cantwell and Forman’s (1993) mesh pattern signifies an approximately equal number of links among the nodes, with no particular node having a higher degree of centrality or connectivity. The candelabra structure identified by Cantwell and Forman (1993) may represent different patterns of spatial connectivity than the spider structure, but the two are topologically and mathematically identical for a given number of nodes or states.

3. Amplification, filtering, and synchronization

3.1. Amplification, filtering, and synchronization in ecological systems

Amplification in general implies positive feedbacks that reinforce ecological changes, and/or dynamical instabilities that

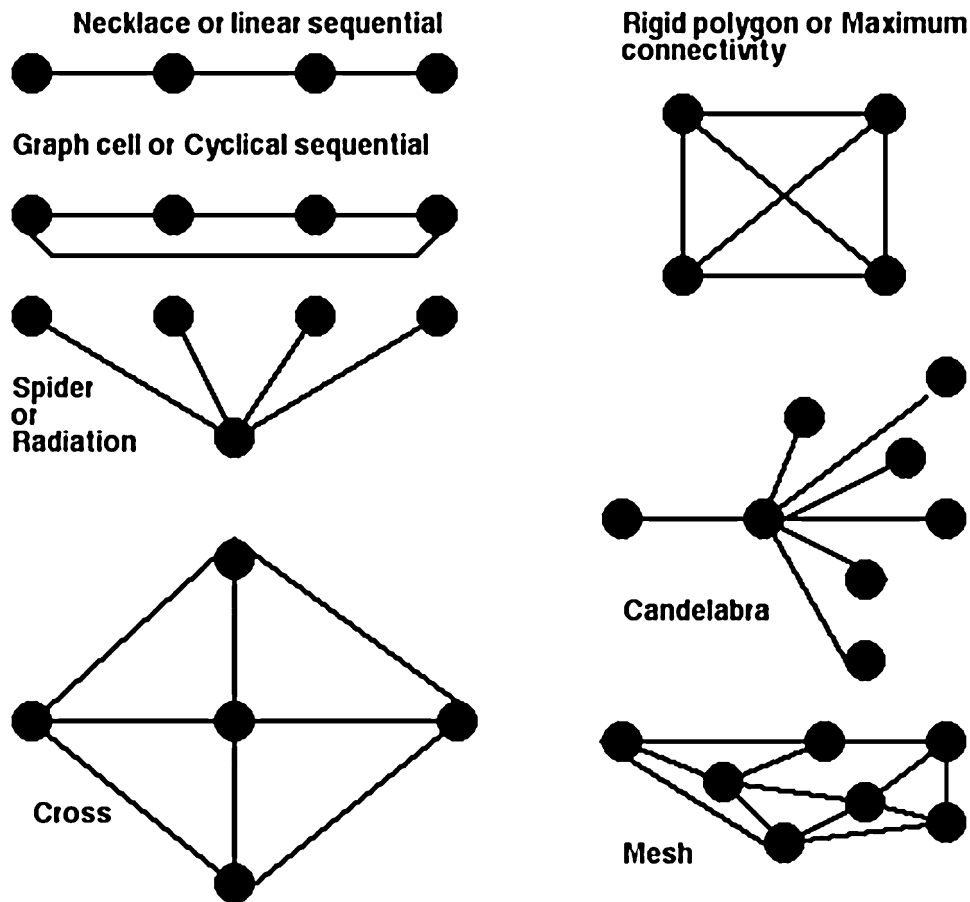


Fig. 1. The seven archetype graph structures.

result in responses disproportionately large relative to disturbances. Filtering refers to phenomena that minimize or diminish effects of changes. Positive feedback amplifier phenomena are well known in ecology (see, e.g., [Wilson and Agnew, 1992](#)). For instance, with respect to shrub invasion of Arctic tundra, climate warming amplifies the dominant driver (nutrient cycling) of shrub expansion dynamics ([Sturm et al., 2005](#)). In their review of global shrub expansion [Naito and Cairns \(2011\)](#) give several other examples of how positive feedbacks amplify effects of shrub invasions. Numerous examples of filtering effects also exist, typically discussed in the framework of ecological resistance and resilience, though ecological resilience theory typically puts more emphasis on irreversible state changes than is the case in STM studies (see reviews in [Gunderson et al., 2010](#), and the discussion of resilience-based STMs by [Briske et al., 2008](#)). An example that explicitly treats filtering in a landscape-scale spatial context is [Wu and Archer's \(2005\)](#) study of topographic amplification and filtering in the semiarid southwestern US. The spatially variable capture and retention of water and nutrients in different landscape patches is an important determinant of and constraint on vegetation patterns, providing a degree of filtering on externally driven ecological changes.

Most examples of positive feedback phenomena and filtering/resilience are “local” in the sense that they reflect effects on specific state transitions. The present paper is concerned with broader-scale amplification or filtering at the landscape or system scale. Local amplification may or may not be associated with landscape-scale amplifier effects. [Perry and Enright \(2002\)](#), for example, showed how amplification via local-scale positive feedback loops may facilitate persistence of either forest or maquis/forest mosaic vegetation cover in New Caledonia. Howev-

er, depending on the landscape flammability, at the landscape scale either amplification (forest to mosaic transitions) or filtering (persistence of forest) may occur.

An example where amplification is not prominent at the local level but does exist at the landscape scale is the response of some salt marshes to sea level rise and storm effects. Local transitions among tidal flats, low (intertidal) marsh, high marsh, and salt pans are generally straightforward and reversible outcomes of geomorphic and hydrochemical forcings. However, at the landscape scale disturbance signals are amplified such that an increasingly complex spatial mosaic of habits and communities develops (see, e.g., [Phillips, 1987](#); [Nyman et al., 1993](#); [van Wesenbeeck et al., 2008](#); [Kim et al., 2009](#)). An example of the reverse is the [Wu and Archer \(2005\)](#) study cited above, where positive feedbacks facilitate grassland-to-shrub transitions locally, but topographically controlled filter effects exist at the landscape scale. [Peters et al. \(2007\)](#) provide a general overview, in the context of changing relationships between ecological patterns and processes, of how amplifier and filter effects may operate at different spatial scales in the same ecosystem or landscape.

Synchronization in ecological networks has heretofore been studied primarily in the context of population ecology. Most of these studies do not explicitly use network or graph theory, but are concerned with the extent to which population changes are synchronous (vs. lagged or temporally independent) in different locations. An exception is [Ranta et al. \(2008\)](#), who studied effects of the structure of dispersal networks on broad-scale synchrony of population fluctuations in populations of several European and North American fauna. In a landscape ecology context [Phillips \(2011\)](#) addressed synchrony as the extent to which state transitions within a deltaic landscape occur more or less

contemporaneously throughout the system, as opposed to a temporal and spatial progression propagating from up- or downstream changes.

Amplification, filtering, and synchronization are all influenced by the extent of structural constraints on the transmission of state changes. Therefore, measures of graph structure indicating the extent of amplification/filtering, synchronization, and structural constraints were applied, as described below.

3.2. Measures of amplification, synchronization, and constraints

Three measures derived from algebraic and spectral graph theory (Biggs, 1994) were applied to the STM graphs. The degree of amplification or filtering of changes within the system is indicated by the *spectral radius*. Fath and colleagues (Fath, 2007; Fath and Haines, 2007; Fath et al., 2007), for instance, have used spectral radius as an indicator of the intensity of cycling in food webs. *Algebraic connectivity* is a widely used measure of the synchronizability of networks (Biggs, 1994). In this application, high synchronization indicates rapid propagation of effects through the network (and vice versa). The *S-metric* is sensitive to the degree to which network nodes are hubs with multiple links. In this study the *S-metric* is an indication of the degree of network structural constraints on state transitions (higher values = lower constraints). The *S-metric* was originally developed by Li et al. (2005) as an indication of the extent to which a system is scale-free.

3.3. Spectral radius

A STM with N states or nodes and the m transitions (edges or links) may be represented as directed (transitions are only possible in one direction along any edge) or undirected (transitions are possible in both directions) graphs. A STM can be treated as an undirected graph if transitions are possible in either direction between any two connected states. A graph is called connected if it is possible to follow a path of one or more edges between any two nodes. STM graphs are all connected, and are generally undirected, though some STMs may include irreversible transitions.

The $N \times N$ adjacency matrix A of an undirected graph has cell values of 1 if the row and column states or nodes are connected, and zero otherwise. A is symmetric for undirected, connected graphs. The adjacency matrix has N eigenvalues λ (which may be complex numbers) such that $\lambda_1 > \lambda_2 > \dots > \lambda_{N-1} > \lambda_N$. The spectral radius is equal to (the real part of) the largest eigenvalue (λ_1). This largest eigenvalue is an important determinant of many graph properties (Restrepo et al., 2007). λ_1 is directly related to the number of loops or cycles in a network. A spectral radius < 1 indicates filtering or damping, so that changes are essentially absorbed by the system. $\lambda_1 > 1$ indicates amplification effects. While spectral radii less than one are unlikely in STMs, higher values indicate stronger ecological ripple effects of externally driven changes, and lower values suggest slower propagation of changes.

The maximum spectral radius for a graph of given number of nodes or states and edges or transitions is

$$\lambda_{1,\max} = \left[\frac{2m(N-1)}{N} \right]^{0.5} \quad (2)$$

Based on this, maximum λ_1 for the archetypal STM structures can be determined based on the number of links (m) associated with a given number of nodes N .

For the necklace/linear sequential pattern, $m = N - 1$, and for the graph cell (cyclical sequential) $m = N$. The radiation (spider and candelabra) patterns also have $m = N - 1$. The cross pattern has $m = 2(N - 1)$. Maximum connectivity (rigid polygon) graphs have

$m = (N^2 - N)/2$. Any graph has $m = Nd/2$, where d is the mean degree (number of links) of each node. The concept of the mesh pattern suggests that this can be constrained based on $2 < d < N - 2$.

3.4. Algebraic connectivity

The second-smallest eigenvalue (λ_{N-1}) of the Laplacian matrix $L(A)$ of the adjacency matrix is called the algebraic connectivity. The entries of Laplacian are:

$$a_{ij} = \begin{cases} \text{deg}(v_i) & \text{if } i = j \\ -1 & \text{if } i \neq j \text{ and } v_i \text{ adjacent to } v_j \\ 0 & \text{otherwise} \end{cases}$$

where $\text{deg}(v_i)$ is the degree of vertex or node i . Algebraic connectivity measures the synchronizability of the system (Biggs, 1994; Duan et al., 2009). It is bounded by the vertex connectivity $\kappa(A)$ and graph diameter D :

$$\frac{4}{ND} \leq \lambda_{N-1} \leq \kappa(A) \quad (3)$$

Vertex connectivity is the minimum number of vertices or nodes that could be removed to disconnect the graph, while diameter is the maximum shortest path (number of links) between any two vertices. Vertex connectivity is bounded by edge connectivity (minimum number of edges that could be removed to disconnect the graph) of A such that $\kappa(A) \leq \text{edge connectivity} \leq \text{minimum degree}$.

Vertex connectivity is $N - 1$ for the maximum connectivity form, 2 for cross and mesh patterns, and 1 for all others. $D = N - 1$ for the linear sequential and $D = N - 2$ for the cyclical sequential cases. For the radiation types, $D = 2$, while $D = 1$ for maximum connectivity. For most conceivable mesh patterns, $2 \leq D \leq N/2$.

3.5. S-metric

The *S-metric* $s(g)$ (Li et al., 2005) applies to simple, undirected, connected graphs with a fixed degree sequence:

$$s(g) = \sum d_i d_j \quad (4)$$

where d is the degree of a given node or state. The fixed degree sequence criterion can be met by constructing the adjacency matrix in order of increasing or decreasing degree along the diagonal. The *S-metric* measures the degree to which the network has a hub-like core, and is maximized when high-degree nodes are connected to other high-degree nodes.

For the archetypal patterns:

$$\text{Necklace (linear sequential): } s(g) = \left\{ \sum_{i=2}^{i=N} [(i-1)N - (i-1)^2] \right\} - N$$

$$\text{Graph cell (cyclical sequential): } s(g) = \sum_{i=2}^{i=N} [(i-1)N - (i-1)^2]$$

$$\text{Spider, candelabra (radiation): } s(g) = (N-1) + (N-2)$$

$$\text{Cross: } s(g) = 12N - 21$$

$$\text{Rigid polygon (maximum connectivity): } s(g) = (N-1)^3$$

$$\text{Mesh: } 12N - 21 \leq s(g) < (N-1)^3$$

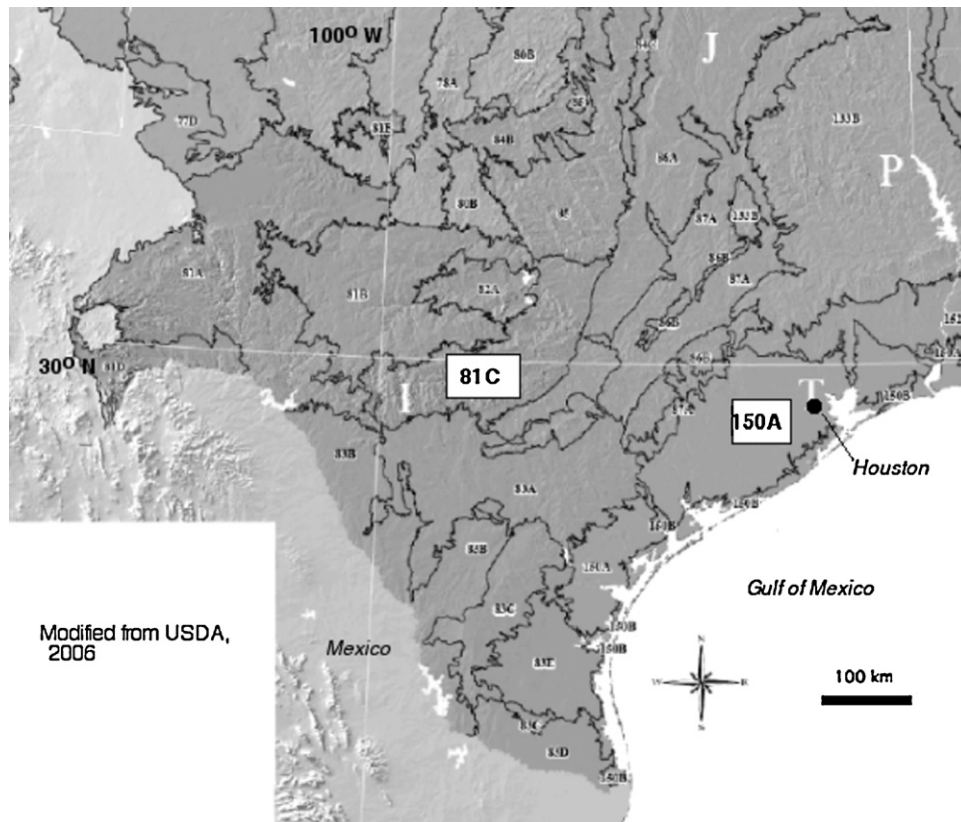


Fig. 2. Location of the Gulf Coastal Prairies (150A) and Edwards Plateau, Eastern Part (081C) Major Land Resource Areas in Texas. Map adapted from detail of the MLRA map for the conterminous USA in USDA (2006).

4. Methods

Analytical expressions for the maximum spectral radius, maximum and minimum algebraic connectivity, and *S*-metric were determined for each archetypal graph structure based on the preceding section. Numerical values or ranges were also calculated for the cases of $N = 5, 10$.

To get some indication of the prevalence of the archetypal structures in real-world systems, STMs were extracted from a U.S. Department of Agriculture (USDA) database, and from the published literature.

By far, most state-and-transition models have been developed for dry environments, ranging from arid to subhumid, and for rangeland and grazing land uses. Many are available in the USDA Ecological Site Descriptions database (<http://esis.sc.egov.usda.gov/Welcome/pgESDWelcome.aspx>). Ecological sites are not specific locations, but environmental types (combinations of soil, vegetation, and geomorphic characteristics) within Major Land Resource Areas (MLRAs). Two USDA MLRAs in Texas were chosen as samples of rangeland STMs – the Gulf Coastal Prairie and the Edwards Plateau, Eastern Part (MLRAs 150A and 081C, respectively; Fig. 2). These were selected because the author is conducting other, field-

based projects in these regions. These MLRAs are described in detail in USDA (2006). All Ecological Site types within these two MLRAs were examined, and the STMs converted to undirected graphs. Following Zweig and Kitchens (2009), it was assumed that all state transitions are reversible, which seems generally consistent with the land use and vegetation histories and ecological phenomena described in the Ecological Site Descriptions. The N, m for each was determined, and the archetypal graph type (or closest match) was identified. An example STM is shown in Fig. 3.

Of course, not all state transitions are equally likely, and the USDA’s STMs distinguish between states *per se*, where transitions involve the crossing of thresholds, and phases within states. Transitions among these phases do not necessarily require threshold crossings (Briske et al., 2008). Because the metrics here are based on the adjacency matrix, they are independent of the weights or probabilities assigned to any given transition.

Relatively few examples of STMs from non-dryland environments are available, but several examples were culled from the literature. These include studies explicitly based on a state-and-transition framework, and others not explicitly STM-based, but which include clearly identified conceptual models of transitions

Table 1
 Values of spectral radius, algebraic connectivity (AC), and the *S*-metric for archetypal STM patterns of a given number of nodes (N).

Graph	Spectral radius (maximum)	AC min	AC max	<i>S</i> -metric
Necklace (linear sequential)	$[2(N-1)^2/N]^{0.5}$	$4/(N^2 - N)$	1	$\{\sum[(i-1)N - (i-1)^2]\} - N$
Graph cell (cyclical sequential)	$[(2N)(N-1)(1/M)]^{0.5}$	$4/(2N)$	1	$4(N-1)$
Spider, candelabra (radiation)	$[2(N-1)^2/N]^{0.5}$	$4/(N^2 - 2N)$	1	$[(N-1) + (N-2)]$
Cross	$\{[4(N-1)^2]/N\}^{0.5}$	$2/N$	2	$12N - 21$
Rigid polygon (maximum connectivity)	$N - 1$	$4/N$	$N - 1$	$(N - 1)^3$
Mesh	$>[4(N-1)^2/N]^{0.5} < N - 1 = [2(Nd/2)(N1)/N]^{0.5}$	$<4/N > 4/(2N)$	2	$\geq 12N - 21 < (N - 1)^3$

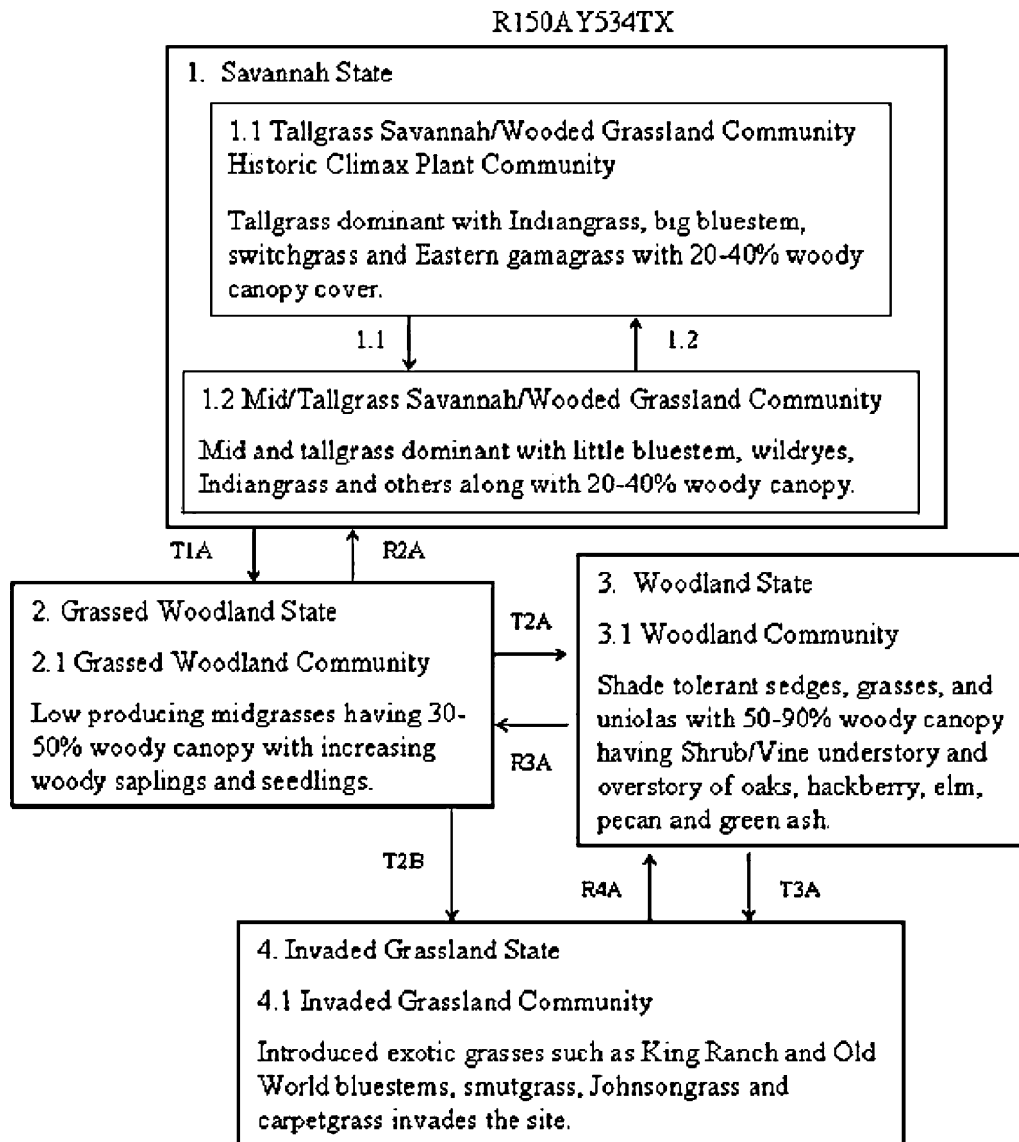


Fig. 3. Example of a STM from the Ecological Site Descriptions database, for the Loamy Bottomland Ecological Site in MLRA 150A.

among vegetation communities, soil types, wetland types, etc. These were examined as described above.

5. Results

5.1. Amplification, synchronization, and constraints

The derived expressions for spectral radius, the range of algebraic connectivity, and $s(g)$ for the archetypal STM patterns are shown in Table 1, and calculated values for the cases of $N = 5, 10$ in Table 2. Several phenomena are readily apparent from these. First, with respect to the maximum λ_1 the necklace or linear sequential pattern is equivalent to the radiation patterns (spider and candelabra). Second, the graph cell or cyclical sequential structure is equivalent to the cross pattern with respect to the lower bound for algebraic connectivity, though the latter has a higher upper bound. The rigid polygon or maximum connectivity pattern has a minimum algebraic connectivity that is always double that of the graph cell.

5.1.1. Amplification

The smallest degree of amplification of state changes, indicated by spectral radius, is associated with the necklace and radiation-

type patterns, with the graph cell type slightly higher. The highest potential λ_1 values are, not surprisingly, associated with the maximally connected rigid polygon pattern, with the cross structure intermediate between the graph cell and rigid polygon. As with all the indices, mesh patterns lie between the cross and rigid polygon values. These rankings remain constant with N , but as the number of states or nodes increases, the proportional differences between the necklace, spider, candelabra, and graph cell decrease, while the difference between these and the cross, mesh, and rigid polygon types increase. This shows that the former group is less sensitive and the latter more sensitive to increases in amplification of state transitions with increasing network size.

5.1.2. Synchronization

Greater synchronization, associated with higher values of algebraic connectivity, signifies more rapid transmission of state transitions through the network. The rigid polygon has the highest values, followed by the cross and mesh patterns. The other patterns all have the same upper bounds, but the lower values are, in descending order, associated with the graph cell, spider/candelabra, and necklace types. Maximum algebraic connectivity values are constant with N for all patterns except the rigid polygon, for

Table 2

Values of spectral radius, algebraic connectivity (AC), and the S-metric for archetypal STM patterns for $N=5$ and $N=10$ (in parentheses).

Graph	Spectral radius	AC min	AC max	S-metric
Necklace (linear sequential)	2.530 (4.025)	0.200 (0.044)	1 (1)	11 (31)
Graph cell (cyclical sequential)	2.828 (4.243)	0.400 (0.200)	1 (1)	16 (36)
Spider, candelabra (radiation)	2.530 (4.025)	0.267 (0.050)	1 (1)	7 (17)
Cross	3.578 (5.692)	0.400 (0.200)	2 (2)	39 (99)
Rigid polygon (maximum connectivity)	4.000 (9.000)	0.800 (0.400)	4 (9)	64 (729)
Mesh	$2.828 \geq \lambda_1 \leq 4.000$ ($4.243 \geq \lambda_1 \leq 9.00$)	$0.32 \leq AC_{min} \leq 4.00$ ($0.08 \leq AC_{min} \leq 0.20$)	2 (2)	$39 \leq s(g) \leq 64$ ($99 \leq s(g) \leq 729$)

Table 3

Characterization of STM graph types for Ecological Sites in MLRA 150A, Gulf Coast Prairies.

Ecological site ID	Name	Graph type	N	m
R150AY526TX	Blackland	Rigid polygon ^a	7	21
R150AY527TX	Clayey Bottomland	Mesh	6	6
		Linked graph cells		
R150AY528TX	Clayplan Prairie	Rigid polygon ^a	6	15
R150AY532TX	Deep Sand	Rigid polygon ^a	4	6
R150AY534TX	Loamy Bottomland	Mesh	6	6
		Linked graph cells		
R150AY535TX	Loamy Prairie	Rigid polygon ^a	7	21
R150AY537TX	Lowland	Rigid polygon ^a	3	3
R150AY540TX	Salty Prairie	Rigid polygon ^a	3	3
R150AY542TX	Sandy Loam	Mesh/rigid polygon	8	24
R150AY543TX	Sandy Prairie	Rigid polygon ^a	7	21
R150AY639TX	Clay Loam	Rigid polygon ^a	6	15
R150AY641TX	Lakebed	Rigid polygon ^a	4	6
R150AY646TX	Tight Sandy Loam	Rigid polygon ^a	7	21
R150AY740TX	Blackland	Rigid polygon ^a	7	21
R150AY741TX	Loamy Prairie	Rigid polygon ^a	7	21

^a Indicates exact match; otherwise indicated graph type is closest approximation.

Table 4

Characterization of STM graph types for Ecological Sites in MLRA 081C, Edwards Plateau, Eastern Part.

Ecological site ID	Name	Graph type	N	m
R081CY356TX	Blackland	Mesh	6	10
R081CY357TX	Clay Loam	Rigid polygon ^a	4	6
R081CY358TX	Deep Redland	Rigid polygon ^a	6	15
R081CY359TX	Gravelly Redland	Rigid polygon ^a	3	3
R081CY360TX	Low Stony Hill	Rigid polygon ^a	5	10
R081CY361TX	Redland	Rigid polygon ^a	6	15
R081CY362TX	Steep Adobe	Rigid polygon ^a	3	3
R081CY363TX	Steep Rocky	Necklace ^a	2	1
R081CY561TX	Loamy Bottomland	Graph cell	4	4
R081CY574TX	Shallow	Rigid polygon ^a	3	3
R081CY699TX	Clayey Bottomland	Rigid polygon ^a	5	10

^a Indicates exact match; otherwise indicated graph type is closest approximation.

Table 5

Characterization of STM graph types for published studies of ecological, pedological, and hydrogeomorphic transitions.

STM	Reference	Graph type	N	m
Forest succession, eastern USA (no disturbance)	Cowles (1911), Clements (1916)	Necklace ^a	5	4
Forest succession, eastern USA (disturbance to climax)	Cowles (1911), Clements (1916)	Graph cell ^a	5	5
Forest succession, eastern USA (subclimax disturbance)	Cowles (1911), Clements (1916)	Graph cell	5	5
Marsh environments, Delaware Bay, New Jersey	Phillips (1987)	Mesh	5	7
Coastal wetland types, Virginia	Brinson et al. (1995)	Necklace	5	4
Soil types, North Carolina Coastal Plain	Phillips et al. (1999)	Mesh	10	13
Forest types, North Carolina Coastal Plain	Phillips (2002)	Graph cell	4	4
Vegetation communities, Island of Capri, shoreline	McIntosh et al. (2003)	Necklace ^a	2	1
Vegetation communities, Island of Capri, coastal	McIntosh et al. (2003)	Radiation	6	7
Vegetation communities, Island of Capri, inland, northern aspect	McIntosh et al. (2003)	Necklace ^a	7	6
Vegetation communities, Island of Capri, inland, southern aspect or plateau	McIntosh et al. (2003)	Graph cell ^a	7	7
Forest types, Victoria, Australia	Czembor and Vesk (2009)	Rigid polygon/cross	4	5
Wetland types, Florida Everglades (landscape scale)	Zweig and Kitchens (2009)	Mesh	17	111
Wet prairie wetland types, Florida Everglades	Zweig and Kitchens (2009)	Graph cell	5	5
Sawgrass marsh wetland types, Florida Everglades	Zweig and Kitchens (2009)	Mesh/graph cell	5	6
Slough wetland types, Florida Everglades	Zweig and Kitchens (2009)	Radiation	6	6
Soil transitions, San Antonio River delta, Texas	Phillips (2011)	Cross	9	18
Soil transitions, Old River avulsion zone, Texas	Phillips (2011)	Graph cell	5	5
Vegetation communities, non-riparian woodlands, SE Australia	Rumpff et al. (2011)	Mesh	7	13

^a Indicates exact match; otherwise indicated graph type is closest approximation.

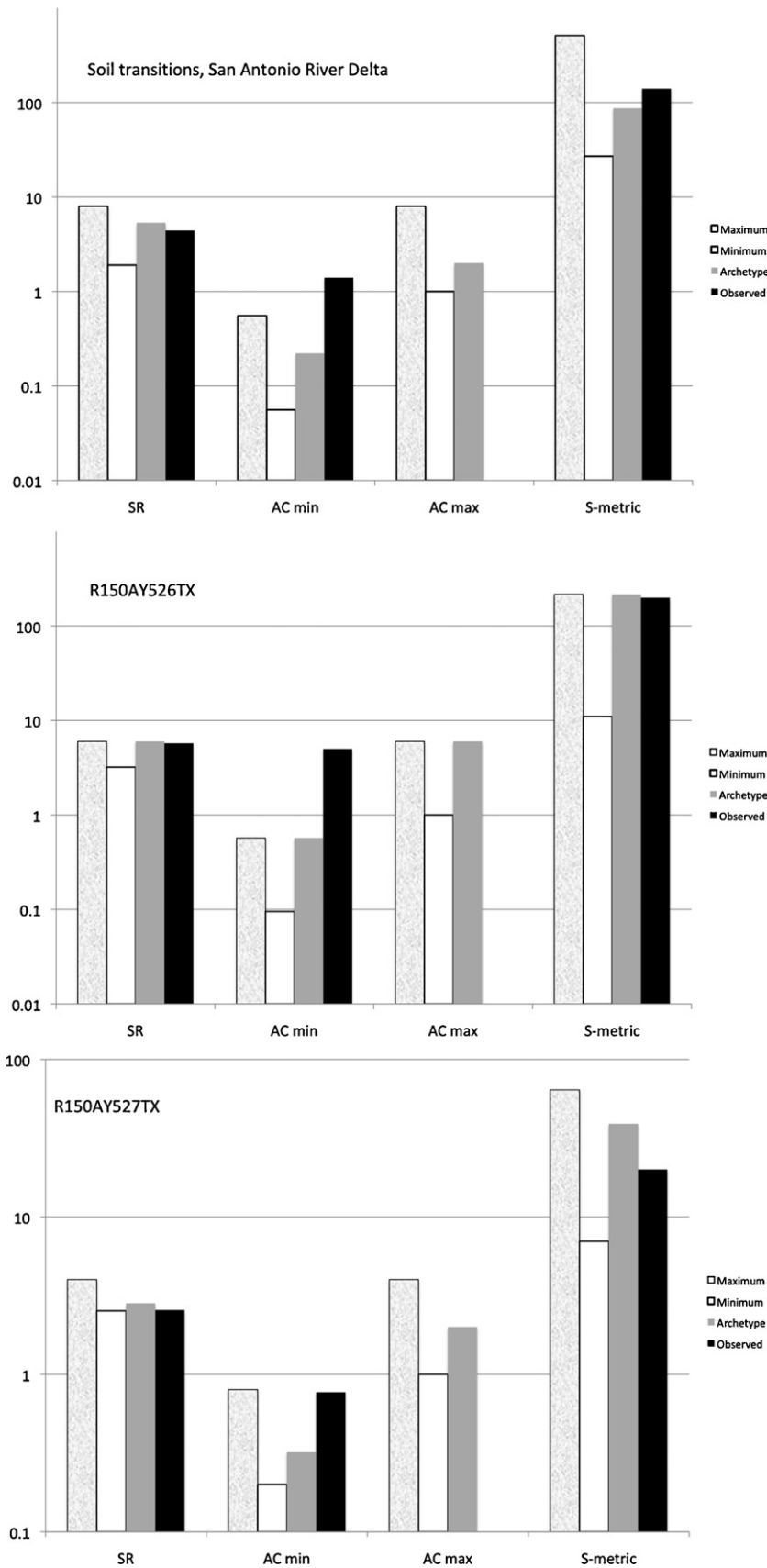


Fig. 4. Observed values of spectral radius (SR), algebraic connectivity (AC) and *S*-metric for three example STMs, compared to maximum and minimum values for the same *N* and for the closest archetypal graph structure. The first is from Phillips (2011), the others are for two ecological land types in the Gulf Coast Prairies Major Land Resource areas. The closest archetypal graph structures are (top to bottom), cross, rigid polygon, and mesh. *N* values are 9, 7, and 5. Note the logarithmic vertical axis, and recall that the analytical values for SR (as opposed to observed) are for the maximum largest eigenvalue.

which it increases linearly with N . The relative rankings of minimum algebraic connectivity do not change with N , but as the size of the network increases all values are shifted downward, and the proportional differences among the patterns are diminished. This reflects the basic principle that for any given pattern of connections, larger networks are harder to synchronize than smaller ones.

5.1.3. Constraints

The degree of system structural constraints to propagation of state transitions, indicated by the S -metric, is highest for the spider/candelabra structure (lowest $s(g)$), followed by the necklace, graph cell, cross, and rigid polygons. Mesh patterns lie between the cross and rigid polygon values. For a given graph pattern, $s(g)$ increases with graph size. This indicates that while larger networks may slow down the propagation of transitions, they provide more options for the eventual transmission of the changes.

5.2. Rangeland graph types

The STM graph types for ecological sites in the Gulf Coastal Prairies MLRA are shown in Table 3. The rigid polygon, maximum connectivity structure characterizes 80% (12 of 15) sites. One other is a dense mesh approaching the rigid polygon, and two others are structures that may be characterized as a linked graph cell. This consists of two graph cell structures with one node in common.

Table 4 shows results for the Edwards Plateau, Eastern Part MLRA. The rigid polygon is also dominant here (8 of 11 ecological sites), with one each of a mesh, necklace, and graph cell.

None of the rangeland STMs has more than eight identified states, with a mean of slightly more than five states each (range 2–8). Classic successional patterns would imply a necklace or graph cell structure, which was found in only two cases. However, one reason STMs were pioneered by range ecologists is that succession-based models were deemed inadequate for these environments (e.g., Westoby et al., 1989; Briske et al., 2005; Bestelmeyer et al., 2009).

5.3. Other STM graph types

Of the 19 examples in Table 5, none are maximum-connectivity structures, though one does approach the rigid polygon. Necklace or graph cell patterns are found in more than half (10 of 19), though some are only approximate matches. It should also be noted that the first three entries were selected to represent classic forest succession models.

The size of the models is similar to the rangeland STMs ($N = 2$ –10), with the exception of one landscape-scale model for which $N = 17$. Excepting the latter, the mean number of states is about 5.7.

Fig. 4 shows a graphical comparison of observed values of spectral radius, algebraic connectivity, and S -metric for three of the STMs described above to the limiting values for STM graphs with the same number of components, and to the values associated with the most closely matching archetype.

6. Discussion and conclusions

6.1. Structural effects on state transitions

The maximum largest eigenvalue increases as (for a given N) one moves from less-connected structures toward the rigid polygon. However, the increase is proportionally small, increasing as m^α , $\alpha < 1$. As long as a graph is connected and $\lambda_1 > 1$, increasing the number of links between nodes or states does not proportionally increase the spectral radius. By contrast, increasing the number of links for a given N produces disproportionately large increases in $s(g)$. For $N > 5$, for instance, the S -metric for the

maximum connectivity case is more than double that of any other structure.

Synchronization is more sensitive to the specific “wiring” of links as opposed to the general graph structure, with relatively small variations among the necklace, graph cell, radiation, and cross patterns for the minimum algebraic connectivity. The cross has a maximum of twice the necklace, graph cell, and radiation patterns. The rigid polygon, however, has a minimum algebraic connectivity at least double that of any structure except a dense mesh, and for $N \geq 5$, the maximum is greater than or equal to twice that of any other pattern, with the difference increasing linearly with N .

Amplification of change will occur if $\lambda_1 > 1$, which is the case for most connected graphs. Amplification increases from structures associated with radiation or succession-type patterns to cross, mesh, and rigid polygon patterns, but may be more sensitive to the specific loop structures in the STM than to the overall pattern.

Dense mesh and rigid polygon structures have much higher synchronization than other patterns, and fewer constraints on change propagation, implying that environments characterized by these types of STMs may be prone to rapid, complex reorganization in response to environmental changes.

While this study is focused on STMs, the methods and findings are potentially applicable to a number of ecological problems amenable to topological representation (Prager and Reiners, 2009). This includes other approaches to the study of multiple and alternative stable states, and to ecological stability domains. Traditional stability analyses are more useful for bistable or two-state systems, but the graph theory approach is useful for systems with more components, and for embedding local stability and resilience analyses into a landscape context (see Section 3.1).

6.2. Implications

Maximum connectivity structures were common in the rangeland STMs examined here, and much less common in STMs for other environments. Are state transitions in non-dryland, non-rangeland environments inherently less connected and characterized by lower spectral radii, algebraic connectivity, and S -metrics? Not necessarily. First, all the rangeland examples relate to vegetation communities, while some of the other STMs deal with soil and hydrogeomorphic transitions that typically operate on slower time scales than vegetation change and must often pass through intermediate states. Second, while the USDA rangeland STMs always consider several possible forcings or disturbances, including climate change, shorter term wet/dry fluctuations, grazing, fire regimes, plantings, and brush management, many of the examples in Table 5 account for only one or two types of change or disturbance.

The results for the STMs in the two MLRAs sampled are broadly consistent with others in the database in the sense that rigid polygon structures are common. This suggests the need for further research to determine the extent to which such high-amplification, high-synchronization patterns characterize networks of ecological state transitions more generally. If this is the case, the implication is that ecological changes triggered by climate and other environmental changes may be more rapid and spatially complex than what would be expected based on succession, gradient, or range of tolerance models.

The findings here are useful for identifying environments at higher risk for rapid, complex reorganizations due to amplification and synchronization of state transitions, with limited constraints. For the typical STM with $N < 10$, this can generally be accomplished by drawing the STM as an undirected graph. The closest archetype can then be identified visually. For larger- N systems, or where more precise quantitative metrics are required, λ_1 , $\lambda(L)_{N-1}$, and $s(g)$ can be calculated and then compared to the values for the archetype structures, using the expressions in Table 1.

This analysis also suggests possibilities for land managers to identify possibilities for either discouraging or enhancing propagation of state changes based on STM structure. By focusing on the facilitation or control of key states or links, managers can either limit change propagation to favor desired states, or facilitate it, for instance to increase habitat diversity.

6.3. Conclusions

The graph structure of state-and-transition models influences the potential amplification, synchronization, and constraints on state changes independently of the ecological dynamics within the individual states. Metrics of these phenomena were determined for seven archetypal graph structures – the necklace, graph cell, candelabra, spider, cross, mesh, and rigid polygon. Radiation-type structures (spider and candelabra) are the least synchronized and most constrained patterns, with the most limited amplification, followed by the other low-connectivity patterns (necklace and graph cell). The maximum-connectivity rigid polygon structure has strongest amplification and synchronization and least constraints, followed by dense mesh and cross patterns. The S -metric is most sensitive to increasing numbers of transitions for a given number of states, and algebraic connectivity also increases at least linearly with the number of links. Spectral radius, however, does not increase as rapidly; as long as a graph is connected, increasing the number of links does not proportionally increase the spectral radius.

The dense mesh and rigid polygon structures, with much higher synchronization than other patterns, and fewer constraints on change propagation, represent environments that may be prone to rapid, complex transitions in response to environmental changes. In two regions of Texas, the rigid polygon structure is very common. To the extent this is common more generally, it suggests that relatively abrupt landscape reorganizations may be more likely than more orderly successions of change along environmental gradients.

Identification of STMs and their network structure is useful for recognizing environments at higher risk for complex reorganization, and for identification of management actions to either retard or facilitate propagation of state changes.

References

Arlinghaus, S.L., Arlinghaus, W.C., Harary, F., 2002. Graph Theory and Geography. An Interactive View. John Wiley, New York.

Bestelmeyer, B., Goolsby, D., Archer, S., 2011. Spatial patterns in alternative states and thresholds: a missing link for management? *Journal of Applied Ecology* 48, 746–757.

Bestelmeyer, B.T., Tugel, A.J., Peacock, D.G., Robinett, D.G., Shaver, P.L., Brown, J.R., Herrick, J.E., Sanchez, H., Havstad, K.M., 2009. State-and-transition models for heterogeneous landscapes: a strategy for development and application. *Rangeland Ecology and Management* 62, 1–15.

Biggs, N., 1994. Algebraic Graph Theory, 2nd ed. Cambridge University Press.

Bode, M., Burrage, K., Possingham, H.P., 2008. Using complex network metrics to predict the persistence of metapopulations with asymmetric connectivity patterns. *Ecological Modelling* 214, 201–209.

Brinson, M.M., Christian, R.R., Blum, L.K., 1995. Multiple states in the sea-level induced transition from terrestrial forest to estuary. *Estuaries* 18, 648–659.

Briske, D.D., Bestelmeyer, B.T., Stringham, T.K., Shaver, P.L., 2008. Recommendations for development of resilience-based state-and-transition models. *Rangeland Ecology and Management* 61, 359–367.

Briske, D.D., Fulendor, S.D., Smeins, F.E., 2005. State-and-transition models, thresholds, and rangeland health: a synthesis of ecological concepts and perspectives. *Rangeland Ecology and Management* 58, 1–10.

Bunn, A.G., Urban, D.L., Keitt, T.H., 2000. Landscape connectivity: a conservation application of graph theory. *Journal of Environmental Management* 59, 265–278.

Burkett, V.R., Wilcox, D.A., Stottlemeyer, R., Barrow, W., Fagre, D., Barron, J., Price, J., Nielsen, J.L., Allen, C.D., Peterson, D.L., Ruggerone, G., Doyle, T., 2005. Nonlinear dynamics in ecosystem response to climate change: case studies and policy implications. *Ecological Complexity* 2, 357–394.

Cantwell, M.D., Forman, R.T.T., 1993. Landscape graphs: ecological modeling with graph theory to detect configurations common to diverse landscapes. *Landscape Ecology* 8, 239–325.

Clements, F.E., 1916. Plant Succession. An Analysis of the Development of Vegetation. Carnegie Institution, Pub. No. 242, Washington.

Cowles, H.C., 1911. The causes of vegetational cycles. *Annals of the Association of American Geographers* 1, 3–20.

Czembor, C.A., Vesik, P.A., 2009. Incorporating between-expert uncertainty into state-and-transition simulation models for forest restoration. *Forest Ecology and Management* 259, 165–175.

Duan, Z.-S., Wang, W.-X., Liu, C., Chen, G.-R., 2009. Are networks with more edges easier to synchronize, or not? *Chinese Physics B* 18, 3122–3130.

Fath, B.D., 2007. Structural food web regimes. *Ecological Modelling* 208, 391–394.

Fath, B.D., Halmes, G., 2007. Cyclic energy pathways in ecological food webs. *Ecological Modelling* 208, 17–24.

Fath, B.D., Scharler, U.M., Ulanowicz, R.E., Hannon, B., 2007. Ecological network analysis: network construction. *Ecological Modelling* 208, 49–55.

Gunderson, L.H., Allen, C.R., Holling, C.S. (Eds.), 2010. Foundations of Ecological Resilience. Island Press, Washington.

Hernstrom, M.A., Merzenich, J., Reger, A., Wales, B., 2007. Integrated analysis of landscape management scenarios using state and transition models in the upper Grande Ronde River subbasin, Oregon, USA. *Landscape and Urban Planning* 80, 198–211.

Iverson, L.R., Prasad, A.M., 2001. Potential changes in tree species richness and forest community types following climate change. *Ecosystems* 4, 186–199.

Iverson, L.R., Prasad, A.M., 2002. Potential redistribution of tree species habitat under five climate change scenarios in the eastern U.S. *Forest Ecology and Management* 155, 205–222.

Kim, D., Cairns, D.M., Bartholdy, J., 2009. Spatial heterogeneity and domain of scale on the Skallingen salt marsh, Denmark. *Geografisk Tidsskrift* 109, 95–112.

Kupfer, J.A., Cairns, D.M., 1996. The suitability of montane ecotones as indicators of global climatic change. *Progress in Physical Geography* 20, 253–272.

Li, L., Alderson, D., Doyle, J.C., Willinger, W., 2005. Towards a theory of scale-free graphs: definition, properties, and implications. Technical Report CIT-CDS-04-006. Engineering & Applied Sciences Division, California Institute of Technology, Pasadena, CA, USA. URL: <http://arxiv.org/pdf/cond-mat/0501169>.

Liang, L., Schwartz, M.D., 2009. Landscape phenology: an integrative approach to seasonal vegetation dynamics. *Landscape Ecology* 24, 465–472.

McIntosh, B.S., Muetzelfeldt, R.I., Legg, C.J., Mazzoleni, St., Csontos, P., 2003. Reasoning with direction and rate of change in vegetation state transition modeling. *Environmental Modelling and Software* 18, 915–927.

Naito, A.T., Cairns, D.M., 2011. Patterns and processes of global shrub expansion. *Progress in Physical Geography* 35, 423–442.

Nyman, J.A., DeLaune, R.D., Roberts, H.H., Patrick, W.H., 1993. Relationship between vegetation and soil formation in a rapidly submerging coastal marsh. *Marine Ecology Progress Series* 96, 264–279.

Padgaham, M., Webb, J.A., 2010. Multiple structural modifications to dendritic ecological networks produce simple responses. *Ecological Modelling* 221, 2537–2545.

Perry, G.L.W., Enright, N.J., 2002. Humans, fire and landscape pattern: understanding a maquis-forest complex, Mont Do, New Caledonia, using a spatial 'state-and-transition' model. *Journal of Biogeography* 29, 1143–1158.

Peters, D.P.C., Bestelmeyer, B.T., Turner, M.G., 2007. Cross-scale interactions and changing pattern-process relationships: consequences for system dynamics. *Ecosystems* 10, 790–796.

Phillips, J.D., 1987. Shoreline processes and establishment of *Phragmites australis* in a coastal plain estuary. *Vegetatio* 71, 139–144.

Phillips, J.D., 1995. Biogeomorphology and landscape evolution: the problem of scale. *Geomorphology* 13, 337–347.

Phillips, J.D., 2002. Global and local factors in earth surface systems. *Ecological Modelling* 149, 257–272.

Phillips, J.D., 2011. Predicting modes of spatial change from state-and-transition models. *Ecological Modelling* 222, 475–484.

Phillips, J.D., Golden, H., Cappiella, K., Andrews, B., Middleton, T., Downer, D., Kelli, D., Padrick, L., 1999. Soil redistribution and pedologic transformations on coastal plain croplands. *Earth Surface Processes and Landforms* 24, 23–39.

Prager, S.D., Reiners, W.A., 2009. Historical and emerging practices in ecological topology. *Ecological Complexity* 6, 160–171.

Ranta, E., Fowler, M.S., Kaitala, V., 2008. Population synchrony in small-world networks. *Proceedings of the Royal Society B* 275, 435–442.

Restrepo, J.G., Ott, E., Hunt, B.R., 2006. Emergence of synchronization in complex networks of interacting dynamical systems. *Physica D* 224, 114–122.

Restrepo, J.G., Ott, E., Hunt, B.R., 2007. Approximating the largest eigenvalue of network adjacency matrices. *Physical Review E* 76. doi:10.1103/PhysRevE.76.056119.

Rumpff, L., Duncan, D.H., Vesik, P.A., Keith, D.A., Wintle, B.A., 2011. State-and-transition modeling for adaptive management of native woodlands. *Biological Conservation*, doi:10.1016/j.biocon.2010.1026.

Ryan, J.G., Ludwig, J.A., McAlpine, C.A., 2007. Complex adaptive landscapes (CAL): a conceptual framework of multi-functional, non-linear ecohydrological feedback systems. *Ecological Complexity* 4, 113–127.

Schaffer, W.M., 1981. Ecological abstraction: the consequences of reduced dimensionality in ecological models. *Ecological Monographs* 51, 383–401.

Sturm, M., Schimel, J., Michaelson, G., Welker, J.M., Oberbauer, S.F., Liston, G.E., Fahnestock, J., Romanovsky, V.E., 2005. Winter biological processes could help convert arctic tundra to shrubland. *Bioscience* 55, 17–26.

- Svenning, J.-C., Skov, F., 2005. The relative roles of environment and history as controls of tree species composition and richness in Europe. *Journal of Biogeography* 32, 1019–1033.
- Tremi, E.A., Halpin, P.N., Urban, D.L., Pratson, L.F., 2008. Modeling population connectivity by ocean currents, a graph-theoretic approach for marine conservation. *Landscape Ecology* 23, 19–36.
- Urban, D.L., Minor, E.S., Tremi, E.A., Schick, R.S., 2009. Graph models of habitat mosaics. *Ecology Letters* 12, 260–273.
- USDA (U.S. Department of Agriculture, Natural Resources Conservation Service), 2006. Land Resource Regions and Major Land Resource Areas of the United States, the Caribbean, and the Pacific Basin. USDA Handbook, p. 296.
- van der Wal, R., 2006. Do herbivores cause habitat degradation or vegetation state transition? Evidence from the tundra. *Oikos* 114, 177–186.
- van Wesenbeeck, B.K., van de Koppel, J., Herman, P.M.J., Bouma, T.J., 2008. Does scale-dependent feedback explain spatial complexity in salt-marsh ecosystems? *Oikos* 117, 152–159.
- Westoby, M., Walker, B., Noy-Meir, I., 1989. Opportunistic management for rangelands not at equilibrium. *Journal of Range Management* 42, 266–274.
- Wilson, J.B., Agnew, A.D.Q., 1992. Positive feedback switches in plant communities. *Advances in Ecological Research* 21, 263–298.
- Wu, X.B., Archer, S.R., 2005. Scale-dependent influence of topography-based hydrologic features on patterns of woody plant encroachment in savanna landscapes. *Landscape Ecology* 20, 733–742.
- Zweig, C.L., Kitchens, W.M., 2009. Multi-state succession in wetlands: a novel use of state and transition models. *Ecology* 90, 1900–1909.